Fourth order accurate compact scheme with group velocity control (GVC)

MA Yanwen (马延文)[1] & FU Dexun (傅德薰)[2]

1. Lab of High Temperature Gasdynamics, Institute of Mechanics, Chinese Academy of Sciences, Beijing 100080, China;
2. Lab of Nonlinear Mechanics, Institute of Mechanics, Chinese Academy of Sciences, Beijing 100080, China
Correspondence should be addressed to Ma Yanwen

Received February 28, 2001

Abstract For solving complex flow field with multi-scale structure higher order accurate schemes are preferred. Among high order schemes the compact schemes have higher resolving efficiency. When the compact and upwind compact schemes are used to solve aerodynamic problems there are numerical oscillations near the shocks. The reason of oscillation production is because of non-uniform group velocity of wave packets in numerical solutions. For improvement of resolution of the shock a parameter function is introduced in compact scheme to control the group velocity. The newly developed method is simple. It has higher accuracy and less stencil of grid points.

Keywords: compact scheme, high resolution of shock, group velocity control.

Recently people pay much attention to the development of higher order accurate schemes. With limited computer resource high order accurate schemes are preferred for solving complex flow field problems because of their smaller amplitude of numerical dissipation and dispersion errors. Many high order accurate schemes have been developed[1—5]. As it is known, solutions of the gas dynamic equations may develop discontinuities even if the initial conditions are smooth. The commonly used high order accurate schemes often give poor results in the presence of the shock[6—12]. There have been a lot of activities geared towards constructing efficient difference schemes with high resolution of the shock. These include TVD, NND and ENO types of schemes. The schemes have been succesfully used for solving practical problems. Usually, rigorous analysis is only done for the scalar one-dimensional nonlinear case although numerical experiments for gasdynamic equations give good results using formal generalization of TVD and ENO types of schemes. Development of the shock capturing finite difference methods of TVD and ENO types is mainly from the view point of mathematics. In the most existing TVD and ENO types of schemes the physical reason of oscillation production is not considered directly. In ref. [1] the relevance of group velocity to the behavior of finite difference model of time-dependent partial differential equations was considered. In ref. [5] the reason of oscillation production in numerical solutions was analysed. According to the group velocity of wave packets, schemes were divided into three groups: slower (SLW), faster (FST) and mixed (MXD). For the schemes from SLW the oscillations in numerical solutions may appear behind the shock; for the schemes from FST oscillations may appear in front of the shocks; and for the schemes from MXD the oscillations may appear in both sides of the shocks. The symmetrical compact schemes in ref. [2] were SLW,

and the upwind compact schemes in refs. [4, 5] were MXD. In the present paper a parameter function is introduced to control the group velocity of wave packets. The compact scheme with GVC is simple. It has smaller stencil of grid points, and the resolution of the shock can be improved much.

1 Compact scheme with free parameter

Consider the following model equation and its semi-difference approximation

$$\frac{\partial u}{\partial t} + \frac{\partial f}{\partial x} = 0, \quad f = cu, \ c = \text{const.} \tag{1.1}$$

$$\frac{\partial u_j}{\partial t} + \frac{F_j}{\Delta x} = 0, \tag{1.2}$$

where $F_j/\Delta x$ is an approximation of $\partial f/\partial x$. The fourth order compact difference approximation is as follows:

$$\frac{1}{6}F_{j+1} + \frac{2}{3}F_j + \frac{1}{6}F_{j-1} = \delta_x^0 f_j, \tag{1.3}$$

where $\delta_x^0 = \frac{1}{2}(\delta_x^+ + \delta_x^-)$, $\delta_x^2 = \delta_x^+\delta_x^-$, $\delta_x^\pm f_j = \mp(f_j - f_{j\pm1})$.

The third order accurate upwind compact difference approximation in ref. [4] was as

$$\frac{2}{3}F_j^\pm + \frac{1}{3}F_{j\mp1}^\pm = \left(\frac{5}{6}\delta_x^\mp + \frac{1}{6}\delta_x^\pm\right)f_j^\pm, \tag{1.4}$$

$$f^\pm = c^\pm u, \ c^\pm = (c \pm |c|)/2. \tag{1.5}$$

We can do the same analysis as it was done in ref. [5], and conclude that scheme (1.2) with (1.3) is SLW, the oscillations for it may appear behind the shock; and the scheme (1.2) with (1.4) is MXD, the oscillations will be mainly in front of the shock with small oscillations behind the shock. We can construct the following difference approximation with a free parameter

$$\frac{1}{6}F_{j+1} + \frac{2}{3}F_j + \frac{1}{6}F_{j-1} - 2\sigma\delta_x^0 F_j = \delta_x^0 f_j - 2\sigma\delta_x^2 f_j. \tag{1.6}$$

For the case $\sigma = 0$ we have the fourth order symmetrical compact difference approximation (1.3). For the case $\sigma = \pm 1/6$, we have the third order upwind compact difference approximation (1.4). For the general case we have

$$\frac{F_j}{\Delta x} = \left(\frac{\partial f}{\partial x}\right)_j + O(\sigma\Delta x^3). \tag{1.7}$$

Here linear dependence of f on u is not required. With initial condition

$$u(x, 0) = \exp(ikx), \tag{1.8}$$

eq. (1.1) has exact solution

$$u(x, t) = \exp[ik(x - ct)]. \tag{1.9}$$

With the same initial condition, eq. (1.2) has the solution

$$u(x_j, t) = \exp\left[-c\frac{k_r}{\Delta x}t\right]\exp\left[ik\left(x_j - c\frac{k_i}{\alpha}t\right)\right], \tag{1.10}$$

where $\alpha = k\Delta x$. The analytical expressions of $k_r(\alpha, \sigma)$ and $k_i(\alpha, \sigma)$ can be obtained easily. The variation of $k_r(\alpha, \sigma)$ with α is given in fig. 1(a). As it is known, the wave packets propa-

gate with group velocity. According to ref. [5] the group velocity is defined by

$$D(\alpha) = \frac{\mathrm{d}k_i(\alpha)}{\mathrm{d}\alpha}. \tag{1.11}$$

For the exact solution of eq. (1.1), $D(\alpha) = 1$. The variations of the group velocity $D(\alpha)$ vs. α are given in fig. 1(b).

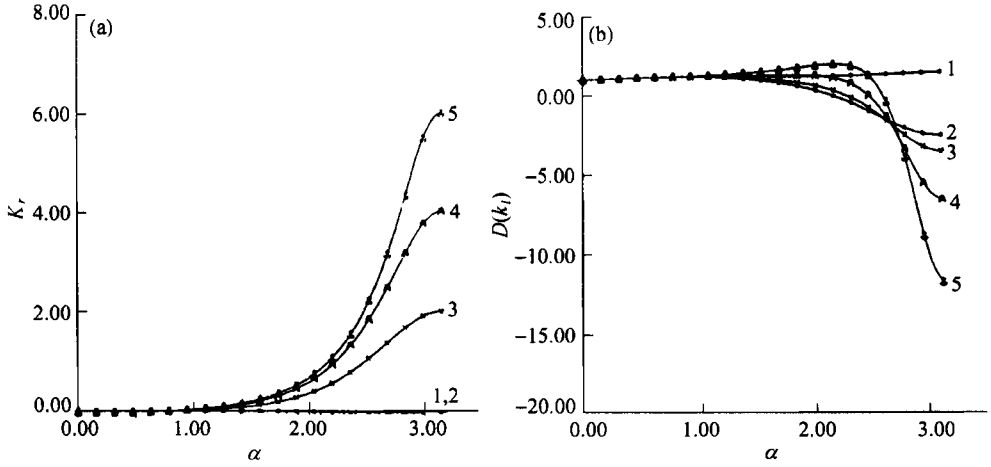

Fig. 1. Variation of k_r and $D(\alpha)$ vs. α. (a) 1, Exact; 2, sigma = 0; 3, sigma = 1/12; 4, sigma = 2/12; 5, sigma = 3/12; (b) 1, exact; 2, sigma = 0; 3, sigma = 1/12; 4, sigma = 2/12; 5, sigma = 3/12.

From fig. 1 it can be seen that the wave component with low wave numbers can be approximated well. With the increasing of the wave number, deviation of numerical solution from the exact solution increases. This is the reason for high-frequency oscillation production in numerical solutions. After careful study it can be seen that for SLW schemes all wave packets in numerical solutions propagate with slower group velocity compared with the exact solution of (1.1). From them some propagate in the same direction as the exact solution (1.1) does, some are standing, and some propagate in the opposite direction. The scheme for the case $\sigma > \sigma_0(\sigma_0 = 0.1291)$ ($c > 0$) is MXD. For MXD scheme the packets with lower and moderate wave numbers have faster group velocity, the wave packets with higher wave numbers have slower group velocity but with small amplitude.

2 Improvement of resolution of shock with GVC

2.1 Scheme construction

We try to use the parameter σ to control the group velocity of wave packets in numerical solutions. For improvement of resolution of the shock it is reasonable to use SLW scheme in front of the shock, and FST scheme behind the shock. Scheme (1.2) with (1.6) for $\sigma = 0$ or small σ is SLW, and it is MXD for large σ. It means that the group velocity of wave packets with very high wave numbers cannot be controlled. Fortunately, the dissipation of scheme increases very fast with the increasing of the parameter σ for high wave number components (fig. 1). The uncontrollable high frequency components can be suppressed by high dissipation.

For controlling the group velocity of wave packets difference approximation (1.6) is reconstructed as follows:

$$\alpha_j^{\pm} F_{j+1}^{\pm} + \beta_j^{\pm} F_j^{\pm} + \gamma_j^{\pm} F_{j-1}^{\pm} = d_j^{\pm}, \tag{2.1}$$

$$\alpha_j^{\pm} = \frac{1}{6} - \sigma_{j+\frac{1}{2}}^{\pm}, \quad \gamma_j^{\pm} = \frac{1}{6} + \sigma_{j-\frac{1}{2}}^{\pm}, \beta_j^{\pm} = \frac{2}{3} - \sigma_{j+\frac{1}{2}}^{\pm} + \sigma_{j-\frac{1}{2}}^{\pm}, \tag{2.2}$$

$$d_j^{\pm} = \delta_x^0 f_j^{\pm} - 2[\sigma_{j+\frac{1}{2}}^{\pm}\delta_x^+ - \sigma_{j-\frac{1}{2}}^{\pm}\delta_x^-]f_j^{\pm},$$

$$\sigma_{j+\frac{1}{2}}^{\pm} = \pm\sigma_0[1 \pm \gamma_0 SS(u_{j+\frac{1}{2}})]\left|\frac{P_{j+1} - P_j}{P_{j+1} + P_j}\right| |c|, \tag{2.3}$$

where $1 \leqslant \sigma_0 \leqslant 2$, $0.8 \leqslant \gamma_0 \leqslant 1$. $SS(u)$ is called shock-structure function and defined as

$$SS(u) = \text{sign}\left(\frac{\partial u}{\partial x} \cdot \frac{\partial^2 u}{\partial x^2}\right). \tag{2.4}$$

Suppose we have N-S shock which is continuous and has large gradient (fig. 2(a)). It is obvious that $SS(u) > 0$ on the left hand side of N-S shock, and $SS(u) < 0$ on the right hand side of N-S shock. The reconstructed scheme (1.2) with (2.1) exhibits SLW property downstream of the shock, and FST property in wide range of wave numbers upstream of the shock.

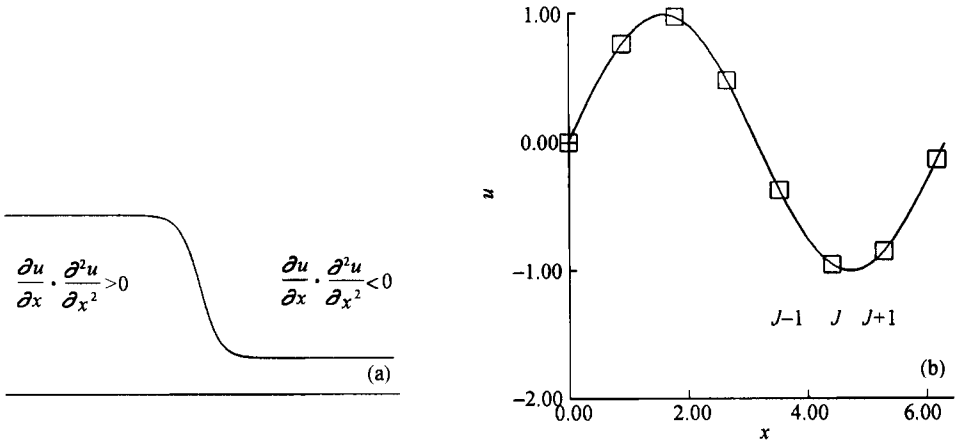

Fig. 2. (a) N-S shock; (b) behavior of a point-function near extremal point.

2.2 Accuracy analysis

From (2.3) it can be seen that $\sigma_{j+\frac{1}{2}} \sim \Delta x$ when the solution is smooth; that is, the newly constructed scheme has fourth order accuracy in the smooth region. In practical application the function $SS(u)$ is approximated as

$$SS(u_{j+\frac{1}{2}}) = \text{sign}[(u_{j+1} - u_j)(u_{j+2} - u_{j+1} - u_j + u_{j-1})]. \tag{2.5}$$

It is obvious that $SS(u)$ changes its sign across the extremal point and inflection point. Suppose $c > 0$ in (2.1) and $\gamma_0 = 1$ in (2.3), and we have a point-function as shown in fig. 2(b). In this case, we have $\sigma_{j+\frac{1}{2}} > 0$ and $\sigma_{j-\frac{1}{2}} = 0$, and the difference approximation has the formula

$$\frac{1}{6}F_{j+1} + \frac{2}{3}F_j + \frac{1}{6}F_{j-1} = \delta_x^0 f_j - \sigma_{j+\frac{1}{2}}[2\delta_x^+ f_j - (F_{j+1} + F_j)]. \tag{2.6}$$

After Taylor series expansion we obtain

$$F_j/\Delta x = \left(\frac{\partial f}{\partial x}\right)_j + O(\sigma\Delta x^2).$$

In the smooth region, $\sigma \sim \Delta x$, and the approximation is third order accurate.

3 Difference approximation for Euler equations

The Euler equations in vector form are as follows:

$$\frac{\partial U}{\partial t} + \frac{\partial f}{\partial x} = 0, \tag{3.1}$$

where $U = [\rho, \rho u, E]^T$, $f = [\rho u, \rho u^2 + p, u(E + p)]^T$,

$$p = \frac{1}{\gamma M_\infty^2}\rho T, \tag{3.2}$$

$$E = \rho\left(c_v T + \frac{u^2}{2}\right). c_v = \frac{1}{\gamma(\gamma - 1)M_\infty^2}, \tag{3.3}$$

M_∞ is the Mach number, γ is the ratio of specific heats. The density ρ, the velocity u, and the temperature T are normalized by ρ_∞, u_∞ and T_∞ respectively, and the pressure p is normalized by $\rho_\infty u_\infty^2$. By using flux splitting we can get a system of equations in split form

$$\frac{\partial U}{\partial t} + \frac{\partial f^+}{\partial x} + \frac{\partial f^-}{\partial x} = 0, \tag{3.4}$$

where $f^\pm = A^\pm U$, $A^\pm = S^{-1}\Lambda^\pm S$, A is the Jacobian matrix, $A = A^+ + A^-$, S is the matrix consisting of eigenvectors of matrix A. The tridiagonal matrix $\Lambda^\pm$ has elements $\lambda_k^\pm = (\lambda_k \pm |\lambda_k|)/2$, $\lambda_1 = u$, $\lambda_2 = u - c$, $\lambda_3 = u + c$, c is the sound speed. $SS(p)$ is used to control the group velocity of wave packets. After spatial discretization we obtain a system of ordinary differential equations which is solved with three-stage Ronge-Kutta method.

In Harten TVD scheme with second order of accuracy in the smooth region five points are used, and the accuracy is reduced at the extremal points. Besides, matrix operations are needed. For the present method also five points are needed but with fourth order of accuracy in the smooth region without matrix operations. The method can be used to solve multi-dimensional problems easily.

4 Numerical experiments

4.1 One-dimensional steady state shock problem

The one-dimensional Euler equations are discretized by using fourth order compact scheme with GVC. In computation the initial conditions are as follows:

$$f = \begin{cases} \text{uniform incoming flow} & 0.00 \leqslant x < 0.45, \\ \text{linear interpolation} & 0.45 \leqslant x < 0.55, \\ \text{R-H relations} & 0.55 \leqslant x \leqslant 1.00, \end{cases} \tag{4.1}$$

where $f = \rho$, u, T, $IN = 101$, $\Delta t/\Delta x = 0.25$, $\sigma_0 = 1$, $\gamma_0 = 0.9$. Two cases are computed. One is for $M_\infty = 2$, and the other one is for $M_\infty = 5$. The results are given in fig. 3. We see that the resolution of the shock is quite good.

4.2 Sod's shock-tube problem

The tube extends from $x = 0$ to $x = 1$ and is divided by 99 equal cells. The gas is initially

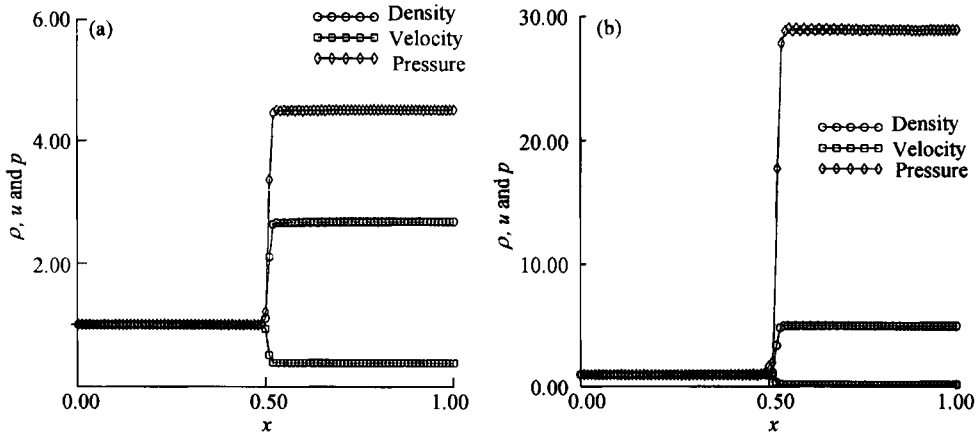

Fig. 3. Steady state shock solutions. (a) $M_\infty = 2$; (b) $M_\infty = 5$.

at rest with $p = \rho = 1$, $u = 0$ in $[0,0.5]$ and $p = 0.1$, $\rho = 0.125$, $u = 0$ in $[0.5,1]$. In computation $\sigma_0 = 1$, $\gamma_0 = 0.9$ are used. The computed results with GVC at $t = 0.14$ are shown in fig. 4.

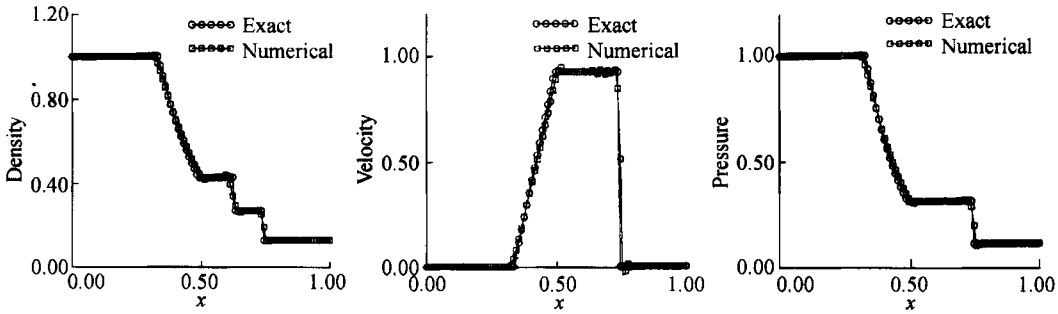

Fig. 4. Solutions of Sod's shock-tube problem at $t = 0.14$.

4.3 Two-dimensional shock reflection

The fourth order compact scheme with GVC which approximates the Euler equations is used to solve two-dimensional shock reflection problem. The incident shock angle $\theta = 29$ and the free stream Mach number is 2.9. The mesh grid system is $X \times Y = 81 \times 41$. The computed pressure distributions at $y = 1/4$, $2/4$ and $3/4$ are given in fig. 5. We can see that the resolution of the shock is much improved.

4.4 Vortex-shock interaction

In ref. [13] a sixth order compact scheme was used to simulate the near field sound generated by vortex-shock interaction with computation grid points 1044×1170. With less grid points oscillations are produced in the numerical solutoins. The same problem is computed here. The inviscid terms in the N-S equations are approximated with the fourth order compact difference relation with GVC, and the viscous terms are approximated with a symmetrical compact difference

relation. Initially a standing shock is located at $x = -0.1$. A pair of vortices are located upstream, and are going through the shock. The computational domain is $[-6, 21]$ in x direction and $[-12, 12]$ in y direction. Near the origin of coordinates $(0,0)$ a uniform fine mesh is used in both x and y directions. In far field from the origin a uniform coarse mesh is used, and between the fine and the coarse meshes the spatial increment is variable. The coordinate transformation is continuous and has continuous first derivative. In computation the uniform incoming flow has Mach number $M_\infty = 1.29$, $\mathrm{Re} = 400$ as used in ref. [13]. The vortex is assumed to have velocity distribution as follows:

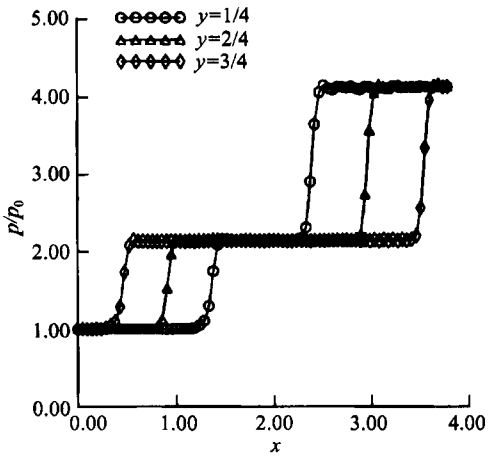

Fig. 5. Pressure distribution at $y = 1/4$, $2/4$ and $3/4$ for shock reflection problem.

$$u_\theta(r) = M_v r \exp[(1 - r^2)/2],$$
$$u_r(r) = 0, \tag{4.2}$$

where r is the distance normalized by the radius of the vortex from the considered point to the center of vortex. The tangential velocity component u_θ and the radial velocity component u_r are normalized by the upstream sound speed a_∞. The Mach number M_v of the vortex is defined by $M_v = u_{\theta\max}/a_\infty$ where $u_{\theta\max}$ is the maximum tangential velocity at $r = 1$. The initial pressure and density distributions are expressed by[13]

$$p(r) = \frac{1}{\gamma}\left[1 - \frac{\gamma - 1}{\gamma} M_v^2 \exp(1 - r^2)\right]^{\frac{\gamma}{\gamma - 1}}, \tag{4.3}$$

$$\rho(r) = \left[1 - \frac{\gamma - 1}{\gamma} M_v^2 \exp(1 - r^2)\right]^{\frac{\gamma}{\gamma - 1}}, \tag{4.4}$$

where $\gamma = 1.4$ denotes the ratio of specific heats. The density and the pressure are normalized by ρ_∞ and $\rho_\infty u_\infty^2$. In present computation $M_v = 0.39$. In fig. 6(a) are given contours of pressure difference $\Delta p = (p - p_s)/p_\infty$, $M_a - 1$ without GVC where p_s is the pressure downstream of the shock without interaction, and M_a is the local Mach number. In fig. 6(b) are given the corresponding results with GVC. The solid lines are for $\Delta p > 0$ and $M_a - 1 > 0$, the dash lines are for $\Delta p < 0$ and $M_a - 1 < 0$. From the computed results it can be seen that the resolution of the shock can be improved much with GVC.

5 Conclusion

(i) According to the reason of oscillation production in numerical solutions the fourth order accurate compact scheme is modified with group velocity control in order to improve the resolution of the shock.

(ii) The new developed scheme is simple, has less stencil of grid points, and is useful to improve the resolution of the shock.

(iii) The new method is used to solve model aerodynamic problems. Numerical experiments show that the resolution of the shock can be improved much.

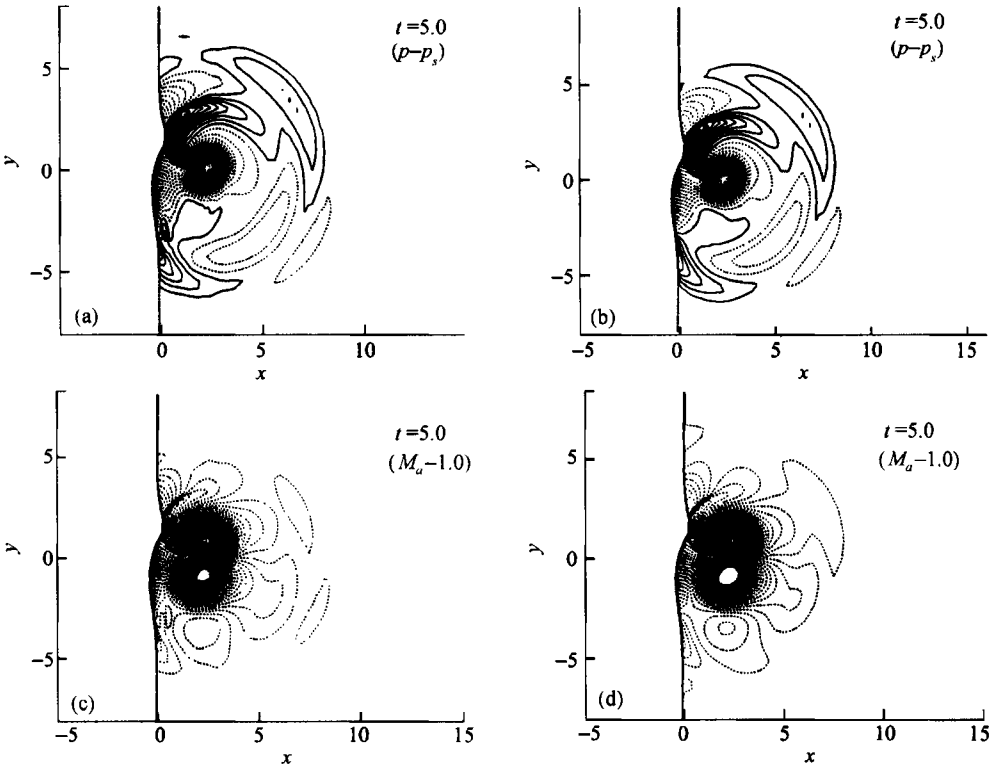

Fig. 6. Contours of pressure difference (a) and $M_a - 1$(c) at $t = 5$ without GVC; contours of pressure difference (b) and $M_a - 1$(d) at $t = 5$ with GVC.

Acknowledgements This work was performed on the computers of the State Kay Laboratory of Scientific and Engineering Computing, the Chinese Academy of Sciences. This work was supporded by the National Natural Science Foundation of China (Grant No. 19972070), "95" Project and 973 Project (Grant No. 1999032805).

References

1. Rai, M. M., Moin, P., Direct simulation of turbulent flow using finite difference schemes, J. Comput. Phys., 1991, 96 (1): 15—53.
2. Lele, S. K., Compact finite difference schemes with spectral-like resolution, J. Comput. Phys., 1992, 13: 16—42.
3. Fu Dexun, Ma Yanwen, High Resolution Schemes, Computational Fluid Dynamics Review (eds. Hafez, M., Oshima, K.), New York: John Wiley & Sons, 1995, 234—250.
4. Fu Dexun, Ma Yanwen, On efficiency and accuracy of numerical methods for solving the aerodynamics equations, numerical methods in fluid mechanics. I, in Proceedings of the International Symposium on Computational Fluid Dynamics (eds. Yasuhara, M., Daiguji, H., Oshima, K.), Nagoya: Japan Society of CFD, 1989, 77—85.
5. Fu Dexun, Ma Yanwen, A high order accurate difference scheme for complex flow fields, J. Comput. Phys., 1997,134: 1—15.
6. Yee, H. C., Warming, R. F., Harten A., Implicit total variation diminishing (TVD) schemes for steady-state calculation, AIAA, 1983, 83—1962.
7. Harten, A., Osher, S., Uniformly high-order accurate non-oscillatory schemes I, SIAM J. Num. Anal., 1987, 24: 279—309.
8. Harten, A., Engquist, B., Chakravarthy, S. R., Uniformly high order accurate essentially non-oscillatory scheme III, J. Compt. Phys., 1987, 71: 231—303.
9. Shu, C. W., TVD uniformlly high-order schemes for conservation law, Math. Comp., 1987, 49(179): 105—121.
10. Ma Yanwen, Fu Dexun, Diffusion analogy and shock capturing for solving the aerodynamic equations, Science in China, Ser. A, 1992, 35(9): 1090—1100.
11. Trefethen, L. N., Group velocity in finite difference schemes, SIAM Review, 1982, 24(2): 113—136.
12. Zhang Hanxin, Discussion of oscillations in numerical solutions near the shock, Acta Aerodynamics Sinica, 1984, (1): 12—19.
13. Inone, O., Hattori, Y., Sound generation by shock-vortex interaction, J. Fluid Mech., 1999, 380: 81—116.